ACS Macro Letters

Letter

pubs.acs.org/macroletters

PIM-1 as a Solution-Processable "Molecular Basket" for CO_2 Capture from Dilute Sources

Simon H. Pang,[†] Melinda L. Jue,[†] Johannes Leisen,[‡] Christopher W. Jones,*[,†,‡] and Ryan P. Lively*[,†]

[†]School of Chemical & Biomolecular Engineering and [‡]School of Chemistry and Biochemistry, Georgia Institute of Technology, Atlanta, Georgia 30332, United States

Supporting Information

ABSTRACT: Rising atmospheric CO_2 levels have triggered recent research into the science of amine materials supported on hard, porous materials such as mesoporous silica or alumina. While such materials can give high CO_2 uptakes and good sorption kinetics, they are difficult to utilize in practical applications due to difficulty in contacting large volumes of CO_2-laden gases with powder materials without significant pressure drops or sorbent attrition. Here, we describe a simple approach based on the impregnation of a permanently microporous polymer, PIM-1, with poly(ethylene imine) (PEI), removing the need for use of the hard oxide. PEI/PIM-1 composites demonstrate comparable performance to more traditionally studied oxide sorbents, with the benefit that PIM-1 is soluble in common solvents, making it eminently more viable for processing into morphologies that can facilitate heat and mass transfer and fabrication into low pressure drop contactors. In addition to adsorption studies performed on a variety of PEI/PIM-1 architectures, spin diffusion NMR studies were performed to suggest that PEI is well-dispersed within the PIM-1, allowing for rapid CO_2 adsorption.

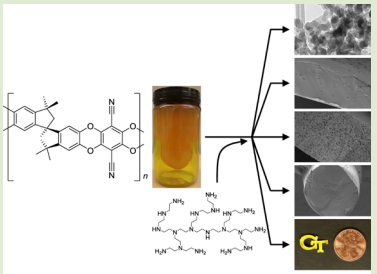

Carbon dioxide capture has received increased attention within the last several decades due to rising atmospheric CO_2 levels. Capturing CO_2 from large point sources such as coal- and gas-fired plants typically involves monoethanolamine-based solutions in commercial scrubbers. These liquid-based processes suffer in their regeneration step due to the high energy penalty imposed by both reversing the CO_2-amine reaction and by unrecoverable latent heat associated with partial evaporation of the water ballast. Moreover, the amines and their degradation products are volatile and can result in additional pollutant emissions from the CO_2 capture unit.[1]

Recent research has focused on solid sorbent materials due to their lower heat capacity, nonevaporative ballast, and potential for high separation efficiency. Silica- and alumina-based materials have been a focal area as a result of their relative ease of preparation. These materials are prepared by chemically grafting an aminosilane[2−6] or physically impregnating an aminopolymer such as poly(ethylene imine) (PEI)[7−20] and have been shown to be useful for dilute CO_2 capture from simulated flue gas (~10−14% CO_2)[21−25] and ultradilute capture from air (400 ppm CO_2).[26−34] However, these materials are typically created as inorganic powders that can be difficult to process and implement at the scales required for real capture applications due to heat and mass transport limitations and high pressure drops. One potential strategy that has been explored is to create porous polymer-inorganic hybrid structures that combine some of the advantages of the polymer (e.g., mechanical integrity) with those of the inorganic material (e.g., high surface area).[35−39] These polymer-inorganic hybrids typically have lower affinity for CO_2 as a result of high loadings (~25−50 wt %) of essentially nonsorptive polymer binder.

Recently, polymers of intrinsic microporosity (PIMs) have garnered attention for applications in a number of important gas separations, among other permanently porous polymers such as porous aromatic frameworks,[40,41] covalent organic frameworks,[42] and porous poly(imide)s.[43] PIM-1 (structure shown in Scheme 1) is the best studied material and has been shown to be useful in membrane separations due to its large permeabilities.[44−46] The spiro centers in the polymer backbone create permanent microporosity in the polymer due to inefficient packing of the polymer chains and relatively low segmental mobility compared to other glassy polymers, resulting in similar pore volume and surface areas for meso-/macropore-free PIM-1 with some traditionally used silica supports such as SBA-15. Thus, the permanent microporosity of PIM-1 can be advantageously utilized by impregnating CO_2-philic molecules (i.e., amines), which we demonstrate here.

An important distinction between inorganic supports and PIM-1 is the solubility of PIM-1 in a select number of common solvents (chloroform, dichloromethane, tetrahydrofuran), allowing it to be processed into a large range of morphologies, including powders, dense coatings, porous membranes, fibers and other designer motifs, as depicted in Scheme 1. All of these structures maintain the permanent microporosity of PIM-1, allowing it to support PEI regardless of final structure; depending on polymer processing conditions, meso-/macropores can be engineered in as well, which can have important

Received: October 30, 2015
Accepted: November 30, 2015
Published: December 7, 2015

DOI: 10.1021/acsmacrolett.5b00775
ACS Macro Lett. 2015, 4, 1415−1419

Scheme 1. PIM-1 Can Be Used As a Support for PEI for Use in CO_2 Capture and Is Solution-Processable, Allowing It to Be Formed into a Wide Range of Topologies, All of Which Retain the Permanent Microporosity Afforded by the Molecular Structure of the Polymer[a]

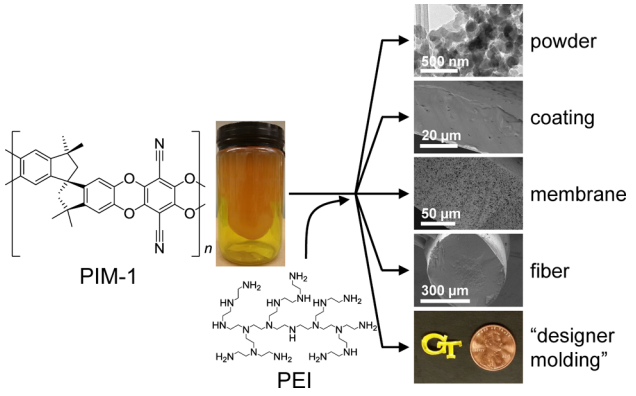

[a]Electron microscopy images show that meso-/macropores can be engineered into the final structure.

and beneficial implications for the heat and mass transfer properties of the final material.

PIM-1 was impregnated with PEI in the range of 5−25 wt % PEI via wet impregnation. The targeted amount of PEI was dissolved in methanol and stirred with PIM-1 powders. The methanol was removed via rotary evaporation and the powders finally dried under vacuum (20 mmHg). The loaded amount of PEI was targeted such that no more than 100% of the original pore volume of the PIM-1 could be filled (based on a PEI density of 1.05 cm^3/g) to encourage PEI to reside inside the pores of PIM-1, rather than on the exterior surface. TGA was used to probe the PEI loading and the decomposition behavior of the composite powder materials. Pure PIM-1 displayed typical decomposition onset at 450 °C in TGA under air; as the loading of PEI was increased up to 21 wt %, decomposition onset shifted to lower temperatures without the appearance of distinct peaks attributable to loss of PEI (Figure S1). Figure 1a shows cryogenic nitrogen physisorption isotherms of these powder composites and mesoporous fibers, and Table 1 summarizes the calculated BET surface area and total pore volume accessible by nitrogen at 77 K.

Pure PIM-1 exhibited a nitrogen adsorption/desorption isotherm with large amounts of microporosity resulting from the inefficient packing of polymer chains.[47,48] Nitrogen physisorption isotherms for pure PIM-1 fibers were similar, indicating that the permanent microporosity is not dependent on final morphology (Figure S2). As expected, PEI filled the pores of PIM-1, resulting in a decrease in the nitrogen-accessible surface area and pore volume; loadings beyond 21 wt % PEI resulted in micropores that were essentially completely occluded by PEI. Based on the pore volume of 0.48 cm^3/g for unmodified PIM-1, the maximum theoretical loading of PEI is 33 wt %. The nearly linear decrease in total pore volume with increased loading suggests that the PEI was well dispersed within the micropores of PIM-1 although a portion of the ultramicropores (pore diameter < 0.7 nm) may have been blocked; the good dispersion of PEI may be assisted by methanol-induced swelling during the impregnation procedure.[49]

Figure 1b shows CO_2 adsorption isotherms for PEI/PIM-1 composites, taken at 35 °C. All isotherms exhibited dual-mode

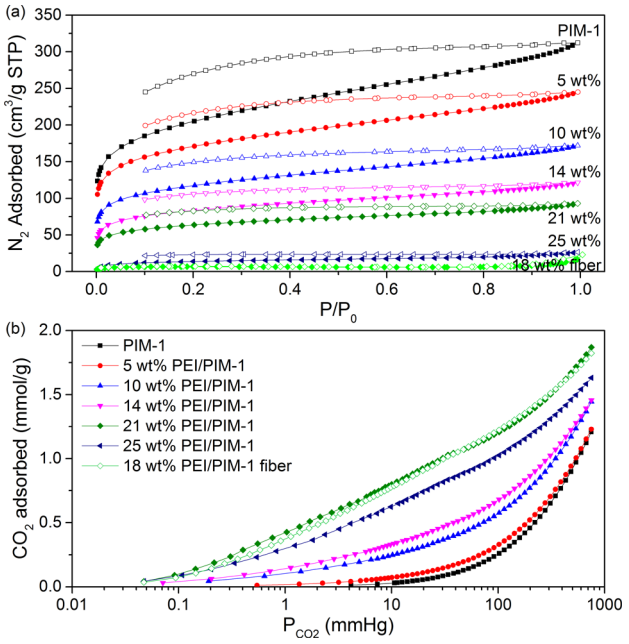

Figure 1. (a) Nitrogen physisorption isotherms at 77 K (adsorption branch shown in filled symbols, desorption branch shown in open symbols) and (b) CO_2 adsorption isotherms at 35 °C for PEI/PIM-1 powders (filled symbols) as a function of PEI loading in weight percent of total mass. PEI/PIM-1 fibers (open symbols) are also shown. Additional data can be found in Figure S2.

sorption behavior typical of glassy polymers, which has also been observed for sorption of a variety of gases in pure PIM-1.[46,49−51] Dual-mode fits and estimated Langmuir and Henry constants are reported in Figure S3. In pure PIM-1, CO_2 exhibited a small amount of Langmuir-type adsorption but predominantly followed Henry's law sorption due to the strong interactions between CO_2 and the nitrile groups on PIM-1.[44]

At the smallest loading of PEI, 5 wt % PEI/PIM-1, the CO_2 adsorption isotherm was changed very slightly compared to the pure PIM-1 isotherm. This was likely due to strong adsorption of PEI on PIM-1 causing most of the amine sites on the PEI to become inaccessible to CO_2. Langmuir adsorption was not significantly increased at these loadings, suggesting that PEI adsorbed in the Langmuir sites that were previously available on PIM-1 and replaced them with Langmuir sites on the PEI. This behavior has also been observed for PEI/MCM-41[8] and PEI/SBA-15[52] at low loadings of PEI.

As PEI loading was further increased to 21 wt %, adsorption on amine Langmuir sites became more important, particularly at low pressures. This region is particularly important for CO_2 capture from flue gas (10−14 vol %) or air (400 ppm) and adsorption capacities in this region reached values in excess of 1 and 0.2 mmol/g, respectively. Beyond 21 wt %, the apparent CO_2 capacity decreased, most likely from the inaccessibility of the amine sites resulting from complete pore blockage by PEI. We hypothesize that at even longer equilibration times such as those used in other literature reports, the CO_2 capacity would appear to be higher than the 21 wt % PEI samples, but these times are impractical for implementation in CO_2 capture applications. Control experiments using gravimetric sorption are shown in Table S1.

Amine efficiencies calculated based on the isotherm capacities from volumetric data are reported in Table 1. This efficiency is calculated as the number of CO_2 molecules

DOI: 10.1021/acsmacrolett.5b00775
ACS Macro Lett. 2015, 4, 1415−1419

Table 1. BET Surface Area (SA) and Total Pore Volume (V_p) Obtained from N_2 Physisorption at 77 K, and CO_2 Pseudo-Equilibrium Uptake Capacities (Q) and Amine Efficiencies for PEI/PIM-1 Powders and Fibers at 35 °C[a]

	SA (m^2/g)	V_p (cm^3/g)	Q_{400} (mmol/g)	N eff.$_{400}$	$Q_{10\%}$ (mmol/g)	N eff.$_{10\%}$
PIM-1	720	0.48	0		0.20	
5 wt %	600	0.38	0.01	0.006	0.27	0.23
10 wt %	410	0.27	0.05	0.023	0.51	0.22
14 wt %	290	0.19	0.08	0.024	0.62	0.19
21 wt %	220	0.14	0.23	0.048	1.15	0.24
25 wt %	50	0.04	0.17	0.030	0.97	0.17
12 wt % fiber	80	0.05	0.12	0.044	0.91	0.33
18 wt % fiber	30	0.03	0.19	0.046	1.16	0.28
25 wt % fiber	30	0.03	0.25	0.042	1.24	0.21
40 wt % SBA-15	80	0.14	1.05[12]	0.11[12]	1.64	0.18

[a]Capacities are reported from the volumetric CO_2 adsorption isotherm experiments at 0.3 and 76 mmHg, corresponding to CO_2 capture from air (Q_{400}) and simulated flue gas ($Q_{10\%}$). The weight percent reported is the fraction of PEI in the total mass of PEI and PIM-1 and is calculated based on the nominal amounts of PEI and PIM-1.

adsorbed per number of nitrogen atoms present in PEI. Under the dry adsorption conditions used, this value has a maximum of 0.38, based on the reported ratio of primary/secondary/tertiary nitrogens of 44:33:23 for the PEI used, assuming that tertiary nitrogen is unable to capture CO_2 and that formation of ammonium carbamate pairs utilizes two nitrogen atoms.[21] This analysis assumes that under dilute CO_2 capture conditions, Henry's law adsorption (in the dual-mode sense) is negligible and that adsorption is strictly due to reaction with amines present on PEI. These amine efficiencies for PEI/PIM-1 in flue gas conditions are comparable to or greater than amine efficiencies obtained for PEI/inorganic composites.[12,16,20]

To demonstrate the versatility of PIM-1 as a support material, PEI-impregnated PIM-1 mesoporous fibers were prepared in an identical fashion to the powders.[37] In contrast to the powders, filled fibers showed lower surface area and pore volume for a given PEI loading, suggesting that PEI was able to reside in the mesopores of these hierarchically porous materials and blocked access to micropores. Despite this, CO_2 capacities were typically high and the materials were able to achieve higher amine efficiencies than their powder counterparts. Nitrogen and CO_2 adsorption isotherms for other fibers can be found in Figures 1 and S2. These fibers can be bundled and used as low pressure drop contactors for CO_2 capture applications.[35]

Solid-state ^1H spin diffusion NMR experiments were performed to probe the microscopic dispersion of PEI within the PIM-1 powder matrix. In these experiments, magnetization on the rigid component (the glassy PIM-1) is filtered out via T_2-relaxation; magnetization on the mobile component (PEI) is retained, causing a nonequilibrium between components. Equilibrium between remaining magnetization states will be reestablished via dipolar coupling causing a magnetization transfer from the mobile component to the rigid component; this can be analyzed in the context of Fickian diffusion. The time required for the magnetization transfer process is related to the characteristic length of the mobile phase, allowing for an estimation of the size of PEI domains within the PIM-1. Additional detail and pulse sequences can be found in refs 53−55 and transverse relaxation curves and spin diffusion curves for 5, 10, and 21 wt % PEI/PIM-1 can be found in Figure S5.

Samples with PEI pore fillings from 20 to 70% exhibited uniform characteristic lengths for spin diffusion and were found to be approximately 2.6 nm. This value closely matches the radius of gyration of the PEI used in this study, though is somewhat larger than the reported average micropore width in PIM-1.[50,56] The small characteristic length is likely a consequence of the confined space, in which PEI resides. The small characteristic length of PEI suggests that in all of these composites, PEI is well-dispersed throughout the PIM-1 matrix and not aggregated, allowing for facile mass transfer.

This finding is in contrast to dispersion of PEI in SBA-15, which has been probed by small-angle neutron scattering.[52] At low loadings, PEI forms a conformal coating on the pore walls due to strong binding between the amine sites and the acidic silica. However, at higher loadings, PEI forms plug-like aggregates due to the relatively wide pore (7−8 nm) of SBA-15 and high surface tension of PEI, resulting in poor dispersion.

To test the applicability of PEI/PIM-1 as a viable CO_2 capture material, temperature swing adsorption tests were performed to evaluate the cyclic stability of the material; the uptake curves are shown in Figure 2a and a summary of the pseudoequilibrium fractional capacities can be found Figure S7a. Over the course of 10 cycles, the adsorbent lost approximately 10% of CO_2 uptake capacity, which is similar to the loss seen in cyclic tests for PEI-loaded SBA-15,[11,22] MCM-41,[14] and PMMA.[57] The capacity loss in all cases is attributed to the formation of urea which irreversibly consumes amine groups,[58] rather than to evaporation of PEI during desorption steps−only 0.3% of the initial mass was lost after 10 cycles. However, as shown in Figure S7b, CO_2 uptake kinetics were not affected by this process. It is important to note that CO_2 capacity lost through urea formation is largely mitigated when these systems are operated in humid feeds, which is likely for many CO_2 capture applications.[22,59] When adsorption on PEI/PIM-1 was operated with humid simulated flue gas, this capacity loss was not observed over several cycles. Moreover, the CO_2 capacity and amine efficiency increased by 40% compared to adsorption from dry simulated flue gas for 10 min of adsorption (Figure S8). This behavior is similar to that observed for silica-supported PEI.[14,22,26]

As seen in Figure 2, adsorption of CO_2 into PEI/PIM-1 followed Fickian uptake behavior as evidenced by the linear CO_2 uptake with $t^{1/2}$ at short time. This behavior can also be seen as the temperature of adsorption is increased from 35 to 80 °C, with the slope of the initial uptake increasing with increasing temperature, as expected for activated diffusion processes, prior to a slow approach to pseudoequilibrium. In comparison, CO_2 adsorption in PEI/SBA-15 quantitatively

DOI: 10.1021/acsmacrolett.5b00775
ACS Macro Lett. 2015, 4, 1415−1419

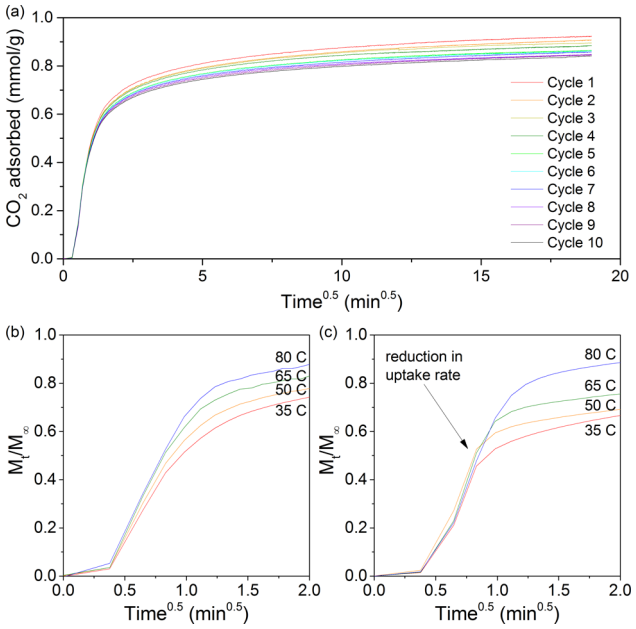

Figure 2. (a) Dynamic CO_2 uptake curves from 10% CO_2/N_2 on 21 wt % PEI/PIM-1 over 6 h of adsorption at 35 °C followed by 2 h of desorption at 110 °C in pure N_2 over the course of ten temperature swing cycles in a TGA. Dynamic CO_2 uptake curves at short time scales as a function of temperature for PEI-loaded (b) PIM-1 and (c) SBA-15 at approximately 70% pore filling. Uptake was normalized against the pseudoequilibrium value reached at 6 h of adsorption.

exhibits non-Fickian behavior. At very short time scales (less than 1 min), the adsorption curves are nearly independent of temperature, suggesting that Knudsen diffusion through the pores of SBA-15 is dominant. However, at longer time scales, the effect of temperature is more apparent, allowing the PEI to become more mobile and allowing CO_2 to diffuse more easily at higher temperature. This effect is less apparent for PEI/PIM-1, corroborating the observation from the spin diffusion NMR experiments that the PEI is well-dispersed in this material. However, increased capacity at higher temperature suggests that not all kinetic limitations have been resolved, highlighting areas for further improvement. The Fickian response exhibited by PEI/PIM-1 is desirable for dilute CO_2 capture applications, as 90% of the pseudoequilibrium capacity is achieved near the "short time" regime. The sharp reduction in uptake rate around M_t/M_∞ = 0.5 for PEI/SBA-15 (Figure 2 and Table S1) is clearly deleterious for CO_2 capture applications where rapid adsorption/desorption cycles are desired to maximize sorbent utility.

This work demonstrates a unique amine-based solid sorbent material composed of PEI and PIM-1 that can be solution-processed into a variety of geometries and used for CO_2 capture from dilute sources. Novel geometries for CO_2 capture contactors (such as hollow fibers and others) allow for major gains in energy efficiency of adsorption systems relative to traditional pellet-based systems due to improved heat mass management, lower pressure drops, and more rapid mass transport.[35−39] The micropores of PIM-1 favor high dispersion of PEI, confirmed by spin diffusion NMR experiments, allowing for quick uptake kinetics and a useful working capacity. The temperature dependence and cyclic stability of PEI/PIM-1 materials was explored, reflecting performance on par with the more commonly studied silica supports. This work suggests that other microporous polymeric materials may be applicable as supports for amine sorbents, warranting further study.

■ ASSOCIATED CONTENT

Supporting Information

The Supporting Information is available free of charge on the ACS Publications website at DOI: 10.1021/acsmacrolett.5b00775.

Materials and procedures, fiber adsorption isotherms, dense film permeation, ^1H spin-diffusion, humid experiments, and other figures as described in the text (PDF).

■ AUTHOR INFORMATION

Corresponding Authors

*E-mail: christopher.jones@chbe.gatech.edu.

*E-mail: ryan.lively@chbe.gatech.edu.

Notes

The authors declare no competing financial interest.

■ ACKNOWLEDGMENTS

This work was supported as part of UNCAGE-ME, an Energy Frontier Research Center funded by the U.S. Department of Energy, Office of Science, Basic Energy Sciences under Award #DE-SC0012577.

■ REFERENCES

(1) Rinker, E. B.; Ashour, S. S.; Sandall, O. C. *Ind. Eng. Chem. Res.* **2000**, *39*, 4346−4356.
(2) Harlick, P. J. E.; Sayari, A. *Ind. Eng. Chem. Res.* **2006**, *45*, 3248−3255.
(3) Sayari, A.; Belmabkhout, Y. *J. Am. Chem. Soc.* **2010**, *132*, 6312−6314.
(4) Belmabkhout, Y.; Serna-Guerrero, R.; Sayari, A. *Adsorption* **2011**, *17*, 395−401.
(5) Sayari, A.; Heydari-Gorji, A.; Yang, Y. *J. Am. Chem. Soc.* **2012**, *134*, 13834−13842.
(6) Bali, S.; Leisen, J.; Foo, G. S.; Sievers, C.; Jones, C. W. *ChemSusChem* **2014**, *7*, 3145−3156.
(7) Xu, X.; Song, C.; Andrésen, J. M.; Miller, B. G.; Scaroni, A. W. *Energy Fuels* **2002**, *16*, 1463−1469.
(8) Xu, X.; Song, C.; Andrésen, J. M.; Miller, B. G.; Scaroni, A. W. *Microporous Mesoporous Mater.* **2003**, *62*, 29−45.
(9) Son, W.-J.; Choi, J.-S.; Ahn, W.-S. *Microporous Mesoporous Mater.* **2008**, *113*, 31−40.
(10) Drese, J. H.; Choi, S.; Lively, R. P.; Koros, W. J.; Fauth, D. J.; Gray, M. L.; Jones, C. W. *Adv. Funct. Mater.* **2009**, *19*, 3821−3832.
(11) Sanz, R.; Calleja, G.; Arencibia, A.; Sanz-Pérez, E. S. *Appl. Surf. Sci.* **2010**, *256*, 5323−5328.
(12) Chaikittisilp, W.; Kim, H. J.; Jones, C. W. *Energy Fuels* **2011**, *25*, 5528−5537.
(13) Heydari-Gorji, A.; Sayari, A. *Chem. Eng. J.* **2011**, *173*, 72−79.
(14) Heydari-Gorji, A.; Belmabkhout, Y.; Sayari, A. *Langmuir* **2011**, *27*, 12411−12416.
(15) Chaikittisilp, W.; Khunsupat, R.; Chen, T. T.; Jones, C. W. *Ind. Eng. Chem. Res.* **2011**, *50*, 14203−14210.
(16) Kuwahara, Y.; Kang, D. Y.; Copeland, J. R.; Brunelli, N. A.; Didas, S. A.; Bollini, P.; Sievers, C.; Kamegawa, T.; Yamashita, H.; Jones, C. W. *J. Am. Chem. Soc.* **2012**, *134*, 10757−10760.
(17) Kuwahara, Y.; Kang, D.-Y.; Copeland, J. R.; Bollini, P.; Sievers, C.; Kamegawa, T.; Yamashita, H.; Jones, C. W. *Chem. - Eur. J.* **2012**, *18*, 16649−16664.
(18) Bali, S.; Chen, T. T.; Chaikittisilp, W.; Jones, C. W. *Energy Fuels* **2013**, *27*, 1547−1554.
(19) Li, K.; Jiang, J.; Tian, S.; Yan, F.; Chen, X. *J. Mater. Chem. A* **2015**, *3*, 2166−2175.

DOI: 10.1021/acsmacrolett.5b00775
ACS Macro Lett. 2015, 4, 1415−1419

(20) Sakwa-Novak, M. A.; Holewinski, A.; Hoyt, C. B.; Yoo, C.-J.; Chai, S.; Dai, S.; Jones, C. W. *Langmuir* **2015**, *31*, 9356−9365.
(21) Hicks, J. C.; Drese, J. H.; Fauth, D. J.; Gray, M. L.; Qi, G.; Jones, C. W. *J. Am. Chem. Soc.* **2008**, *130*, 2902−2903.
(22) Heydari-Gorji, A.; Sayari, A. *Ind. Eng. Chem. Res.* **2012**, *51*, 6887−6894.
(23) Fauth, D. J.; Gray, M. L.; Pennline, H. W.; Krutka, H. M.; Sjostrom, S.; Ault, A. M. *Energy Fuels* **2012**, *26*, 2483−2496.
(24) Wang, X.; Ma, X.; Song, C.; Locke, D. R.; Siefert, S.; Winans, R. E.; Möllmer, J.; Lange, M.; Möller, A.; Gläser, R. *Microporous Mesoporous Mater.* **2013**, *169*, 103−111.
(25) Qi, G.; Fu, L.; Giannelis, E. P. *Nat. Commun.* **2014**, *5*, 5796.
(26) Belmabkhout, Y.; Serna-Guerrero, R.; Sayari, A. *Chem. Eng. Sci.* **2010**, *65*, 3695−3698.
(27) Choi, S.; Gray, M. L.; Jones, C. W. *ChemSusChem* **2011**, *4*, 628−635.
(28) Choi, S.; Drese, J. H.; Eisenberger, P. M.; Jones, C. W. *Environ. Sci. Technol.* **2011**, *45*, 2420−2427.
(29) Wurzbacher, J. A.; Gebald, C.; Steinfeld, A. *Energy Environ. Sci.* **2011**, *4*, 3584−3592.
(30) Goeppert, A.; Czaun, M.; May, R. B.; Prakash, G. K. S.; Olah, G. A.; Narayanan, S. R. *J. Am. Chem. Soc.* **2011**, *133*, 20164−20167.
(31) Stuckert, N. R.; Yang, R. T. *Environ. Sci. Technol.* **2011**, *45*, 10257−10264.
(32) Brunelli, N. A.; Didas, S. A.; Venkatasubbaiah, K.; Jones, C. W. *J. Am. Chem. Soc.* **2012**, *134*, 13950−13953.
(33) Didas, S. A.; Kulkarni, A. R.; Sholl, D. S.; Jones, C. W. *ChemSusChem* **2012**, *5*, 2058−2064.
(34) Wang, J.; Huang, H.; Wang, M.; Yao, L.; Qiao, W.; Long, D.; Ling, L. *Ind. Eng. Chem. Res.* **2015**, *54*, 5319−5327.
(35) Lively, R. P.; Chance, R. R.; Kelley, B. T.; Deckman, H. W.; Drese, J. H.; Jones, C. W.; Koros, W. J. *Ind. Eng. Chem. Res.* **2009**, *48*, 7314−7324.
(36) Lively, R. P.; Leta, D. P.; DeRites, B. A.; Chance, R. R.; Koros, W. J. *Chem. Eng. J.* **2011**, *171*, 801−810.
(37) Labreche, Y.; Lively, R. P.; Rezaei, F.; Chen, G.; Jones, C. W.; Koros, W. J. *Chem. Eng. J.* **2013**, *221*, 166−175.
(38) Labreche, Y.; Fan, Y.; Rezaei, F.; Lively, R. P.; Jones, C. W.; Koros, W. J. *ACS Appl. Mater. Interfaces* **2014**, *6*, 19336−19346.
(39) Fan, Y.; Labreche, Y.; Lively, R. P.; Koros, W. J.; Jones, C. W. *AIChE J.* **2014**, *60*, 3878−3887.
(40) Yuan, D.; Lu, W.; Zhao, D.; Zhou, H.-C. *Adv. Mater.* **2011**, *23*, 3723−3725.
(41) Ben, T.; Qiu, S. *CrystEngComm* **2013**, *15*, 17−26.
(42) Côté, A. P.; Benin, A. I.; Ockwig, N. W.; O'Keeffe, M.; Matzger, A. J.; Yaghi, O. M. *Science* **2005**, *310*, 1166−1170.
(43) Ritter, N.; Senkovska, I.; Kaskel, S.; Weber, J. *Macromol. Rapid Commun.* **2011**, *32*, 438−443.
(44) Budd, P. M.; Msayib, K. J.; Tattershall, C. E.; Ghanem, B. S.; Reynolds, K. J.; McKeown, N. B.; Fritsch, D. *J. Membr. Sci.* **2005**, *251*, 263−269.
(45) Mason, C. R.; Maynard-Atem, L.; Al-Harbi, N. M.; Budd, P. M.; Bernardo, P.; Bazzarelli, F.; Clarizia, G.; Jansen, J. C. *Macromolecules* **2011**, *44*, 6471−6479.
(46) Li, P.; Chung, T. S.; Paul, D. R. *J. Membr. Sci.* **2013**, *432*, 50−57.
(47) Budd, P. M.; Elabas, E. S.; Ghanem, B. S.; Makhseed, S.; McKeown, N. B.; Msayib, K. J.; Tattershall, C. E.; Wang, D. *Adv. Mater.* **2004**, *16*, 456−459.
(48) Budd, P. M.; Ghanem, B. S.; Makhseed, S.; McKeown, N. B.; Msayib, K. J.; Tattershall, C. E. *Chem. Commun.* **2004**, *2*, 230.
(49) Jue, M. L.; McKay, C. S.; McCool, B. A.; Finn, M. G.; Lively, R. P. *Macromolecules* **2015**, *48*, 5780−5790.
(50) McKeown, N. B.; Gahnem, B.; Msayib, K. J.; Budd, P. M.; Tattershall, C. E.; Mahmood, K.; Tan, S.; Book, D.; Langmi, H. W.; Walton, A. *Angew. Chem., Int. Ed.* **2006**, *45*, 1804−1807.
(51) Bushell, A. F.; Budd, P. M.; Attfield, M. P.; Jones, J. T. A.; Hasell, T.; Cooper, A. I.; Bernardo, P.; Bazzarelli, F.; Clarizia, G.; Jansen, J. C. *Angew. Chem., Int. Ed.* **2013**, *52*, 1253−1256.
(52) Holewinski, A.; Sakwa-Novak, M. A.; Jones, C. W. *J. Am. Chem. Soc.* **2015**, *137*, 11749−11759.
(53) Clauss, J.; Schmidt-Rohr, K.; Spiess, H. W. *Acta Polym.* **1993**, *44*, 1−17.
(54) Mellinger, F.; Wilhelm, M.; Spiess, H. W. *Macromolecules* **1999**, *32*, 4686−4691.
(55) Leisen, J.; Beckham, H. W.; Sharaf, M. A. *Macromolecules* **2004**, *37*, 8028−8034.
(56) Heuchel, M.; Fritsch, D.; Budd, P. M.; McKeown, N. B.; Hofmann, D. *J. Membr. Sci.* **2008**, *318*, 84−99.
(57) Jung, H.; Jo, D. H.; Lee, C. H.; Chung, W.; Shin, D.; Kim, S. H. *Energy Fuels* **2014**, *28*, 3994−4001.
(58) Drage, T. C.; Arenillas, A.; Smith, K. M.; Snape, C. E. *Microporous Mesoporous Mater.* **2008**, *116*, 504−512.
(59) Didas, S. A.; Zhu, R.; Brunelli, N. A.; Sholl, D. S.; Jones, C. W. *J. Phys. Chem. C* **2014**, *118*, 12302−12311.

DOI: 10.1021/acsmacrolett.5b00775
ACS Macro Lett. 2015, 4, 1415−1419